THE JOURNAL OF BIOLOGICAL CHEMISTRY VOL. 280, NO. 47, pp. 39637–39643, November 25, 2005
Printed in the U.S.A.

Functional Analysis of Conserved Polar Residues in Vc-NhaD, Na^+/H^+ Antiporter of *Vibrio cholerae*[*] [S]

Received for publication, August 24, 2005, and in revised form, September 23, 2005 Published, JBC Papers in Press, September 26, 2005, DOI 10.1074/jbc.M509328200

Rahim Habibian[‡], Judith Dzioba[‡], Jeannie Barrett[‡], Michael Y. Galperin[§1], Peter C. Loewen[‡], and Pavel Dibrov[‡2]

From the [‡]Department of Microbiology, University of Manitoba, Winnipeg, Manitoba R3T 2N2, Canada and [§]National Center for Biotechnology Information, National Library of Medicine, National Institutes of Health, Bethesda, Maryland 20894

Vc-NhaD is a Na^+/H^+ antiporter from *Vibrio cholerae* with a sharp maximum of activity at pH ~ 8.0. NhaD homologues are present in many bacteria as well as in higher plants. However, very little is known about structure-function relations in NhaD-type antiporters. In this work 14 conserved polar residues associated with putative transmembrane segments of Vc-NhaD have been screened for their possible role in the ion translocation and pH regulation of Vc-NhaD. Substitutions S150A, D154G, N155A, N189A, D199A, T201A, T202A, S389A, N394G, S428A, and S431A completely abolished the Vc-NhaD-mediated Na^+-dependent H^+ transfer in inside-out membrane vesicles. Substitutions T157A and S428A caused a significant increase of apparent K_m values for alkali cations, with the K_m for Li^+ elevated more than that for Na^+, indicating that Thr-157 and Ser-428 are involved in alkali cation binding/translocation. Of six conserved His residues, mutation of only His-93 and His-210 affected the $Na^+(Li^+)/H^+$ antiport, resulting in an acidic shift of its pH profile, whereas H93A also caused a 7-fold increase of apparent K_m for Na^+ without affecting the K_m for Li^+. These data suggest that side chains of His-93 and His-210 are involved in proton binding and that His-93 also contributes to the binding of Na^+ ions during the catalytic cycle. These 15 residues are clustered in three distinct groups, two located at opposite sides of the membrane, presumably facilitating the access of substrate ions to the third group, a putative catalytic site in the middle of lipid bilayer. The distribution of these key residues in Vc-NhaD molecule also suggests that transmembrane segments IV, V, VI, X, XI, and XII are situated close to one another, creating a transmembrane relay of charged/polar residues involved in the attraction, coordination, and translocation of transported cations.

Sodium proton antiporters are universal secondary ion transporters in bacteria. Typically, they expel toxic Na^+ and Li^+ ions from the cytoplasm at the expense of the proton motive force, thus playing an important role in cytoplasmic Na^+ and pH homeostasis and providing energy for Na^+ symports (for review, see Refs. 1–4). The Na^+/H^+ antiport in a bacterial cell is often mediated by antiporters of different types working in concert. Major enterobacterial antiporters, Ec-NhaA (5) and Ec-NhaB (6), have been extensively characterized in *Escherichia coli* (see Refs. 7–19; for review also see Ref. 4, and for recent progress see Refs. 20–23). The genome of pathogenic *Vibrio cholerae* encodes as many as six putative structural genes of Na^+/H^+ antiporters (24). The physiological basis for such apparent redundancy could be in part explained by recent findings of additional, predominantly regulatory functions of certain bacterial Na^+/H^+ antiporters affecting processes such as antibiotic efflux (25), the transcription of the Pho operon (26), the initiation of sporulation (27), and endospore germination (28).

Studying Na^+/H^+ antiport in *V. cholerae*, we have cloned a new Na^+/H^+ antiporter from *V. cholerae*, Vc-NhaD, and expressed it in its functional form in the ΔNhaAΔNhaB strain of *E. coli* (29). A distinctive feature of Vc-NhaD is its pH dependence with a sharp maximum of activity at pH ~ 8.0 (29–30). This distinguishes Vc-NhaD from other major enterobacterial antiporters. Indeed, Ec-NhaB from *E. coli* is pH-independent, whereas the activity of Ec-NhaA gradually increases upon pH shift from 7.0 to 8.0, reaching a plateau (9). Curiously, homologous NhaD from *Vibrio parahaemolyticus* exhibits pH dependence similar to Ec-NhaA rather than Vc-NhaD (31).

The Na^+/H^+ antiporters of NhaD type are widely distributed in nature, being found in genomes of pathogenic vibrios, nitrogen-fixing symbionts, magnetotactic cocci and photosynthetic bacteria as well as in higher plants (Fig. 1). In obligate intracellular parasites of *Chlamydia* genus, NhaD serves as a sole Na^+/H^+ antiporter (32–33). However, very little is known about the molecular mechanisms of cation exchange mediated by these proteins. In the absence of a detailed crystal structure, identification of functionally important residues in antiporters by site-directed mutagenesis remains one of the most informative approaches. Because Na^+/H^+ antiporters are exchanging cations, negatively charged residues are obvious primary targets for mutagenesis (see for example Refs. 18 and 23). In our previous work we found that mutation of three polar residues, Asp-344, Thr-345 (TMS[3] X and loop IX-X), and Asp-393 (within TMS XI) severely affects the Na^+-dependent proton transfer mediated by Vc-NhaD (30). In the present study we extended these observations by mutating Vc-NhaD residues that are conserved in NhaD homologues from different organisms (see Fig. 1). In particular, the following questions were addressed. (i) Are polar residues Ser-389, Ser-390, and Asn-394 surrounding Asp-393 in TMS XI functionally important as well? (ii) Do the distant conserved polar residues associated with TMS V and VI (Asp-154, Thr-157, Asp-199, Thr-201, Thr-202) affect the function of Vc-NhaD? (iii) Are any of the conserved His residues involved in the pH response of Vc-NhaD, such as His-225 in Ec-NhaA (15–16)? (iv) How would the substitution of all Cys residues by serines affect the activity?

Here we report the identification of three distinct clusters of functionally important polar residues dispersed through the protein. Cluster

* This research was supported by grants from Natural Sciences and Engineering Research Council of Canada (to P. C. L., P. D., R. H., and J. D.) and the Canada Research Chair Program (to P. C. L.). The costs of publication of this article were defrayed in part by the payment of page charges. This article must therefore be hereby marked "*advertisement*" in accordance with 18 U.S.C. Section 1734 solely to indicate this fact.

[S] The on-line version of this article (available at http://www.jbc.org) contains a supplemental table.

[1] Supported by the Intramural Research Program at the National Library of Medicine, National Institutes of Health.

[2] To whom correspondence should be addressed: Dept. of Microbiology, University of Manitoba, Fort Garry campus, Rm. 425 Buller Bldg., Winnipeg, Manitoba R3T 2N2 Canada. Tel.: 204-474-8059; Fax: 204-474-7603; E-mail: dibrovp@ms.umanitoba.ca.

[3] The abbreviations used are: TMS, transmembrane segment; Ec-NhaA and Ec-NhaB, Na^+/H^+ antiporters of NhaA type and NhaB type from *E. coli*, respectively; Vc-NhaD, Na^+/H^+ antiporter of NhaD type from *V. cholerae*; ΔpH, pH difference across the membrane; PBS, phosphate-buffered saline.

1 is associated with TMS IV-VI at the periplasmic side of the protein, cluster 2 is at the opposite side facing cytoplasm (TMS X), and cluster 3 in TMS XI-XII is located in the middle of the transmembrane segments. Together with residues His-93 and His-210, which control the pH profile of the antiport and its affinity to alkali cations, these clusters may form a transmembrane relay of charged/polar residues involved in the attraction, coordination, and translocation of transported ions in a striking similarity to the recently reported structure of phylogenetically distant Ec-NhaA (22).

EXPERIMENTAL PROCEDURES

Materials—All chemicals were from Fisher or Sigma. Restriction nucleases were from Invitrogen, MBI Fermentas, or New England Biolabs.

Bacterial Strains and Culture Conditions—The Na^+/H^+ antiporter-deficient (*mel*BLid, ΔNhaB1, *cam*^{R}, ΔNhaA1, *kan*^{R}, Δ*lac*ZY, *thr*1) strain of *E. coli*, EP432 was kindly provided by Dr. E. Padan (Hebrew University of Jerusalem, Jerusalem, Israel). For routine cloning and plasmid construction, DH5α (United States Biochemical Corp.) was used as the host. If not indicated otherwise, cells were grown aerobically at 37 °C in modified L broth (LBK) in which NaCl was replaced by KCl (7). All transformants were grown in media supplemented with 100 μg/ml ampicillin.

Site-directed Mutagenesis—Site-directed mutagenesis was performed with the QuikChange site-directed mutagenesis kit (Stratagene) as recommended by the manufacturer. The mutagenic oligonucleotide primers were designed to create or remove specific restriction enzyme sites (listed in the supplemental table). As a template for mutagenesis, the plasmid pBLDL (pBluescript II KS+ (Stratagene) containing the *nhaD* gene together with the 300-bp-long 5′- and 230-bp-long 3′-flanking sequences as a 1837-bp EcoRI-BamHI insert) was used (29). Mutated plasmid DNA was isolated from selected transformant clones and digested by appropriate restriction enzymes to check for the presence of desired mutation. The minimal *nhaD* fragments containing the target mutation were then excised and used to replace the respective sequences in the original (non-mutated) pBLDL. Fidelity of all final mutated versions of *nhaD* in pBLDL was verified by DNA sequencing.

Isolation of Membrane Vesicles and Assay of Na^+/H^+ Antiport Activity—Inside-out membrane vesicles were obtained by passing a bacterial suspension through a French press (Aminco) and assayed for Na^+/H^+ antiport activity as described previously (29–30). Protein content in membrane vesicles was determined by the Bio-Rad detergent compatible protein assay kit. The Na^+/H^+ antiporter activity was registered by the acridine orange fluorescence dequenching. Aliquots of vesicles (200 μg of protein) were resuspended in 2 ml of a medium containing 100 mM KCl, 250 mM sucrose, 10 mM $MgSO_4$, 0.5 μM acridine orange, and 50 mM Hepes-Tris buffer adjusted to the indicated pH. Respiration-dependent formation of the ΔpH was initiated by the addition of 10 mM Tris-D-lactate, and the resulting quenching of acridine orange fluorescence was monitored with the Shimadzu RF-1501 spectrofluorophotometer (excitation at 492 nm and emission at 528 nm). Na^+/H^+ antiporter activity was estimated based on its ability to dissipate the established ΔpH upon the addition of the indicated concentrations of NaCl or LiCl (10 mM in the pH-profile determination; 0.5–50 mM for the determination of half-maximal effective concentration). The antiport activities are expressed as percent restoration of the lactate-induced fluorescence quenching.

In Silico Analysis of Vc-NhaD—NhaD homologues in various organisms were identified through a BLASTP (34) search against the NCBI (Bethesda, MD) nonredundant protein database. A partial alignment showing the conserved polar residues located within or associated with putative transmembrane segments as well as conserved His and Cys residues is shown in Fig. 1. Putative membrane topology model of NhaD from *V. cholerae* (Fig. 1*B*) was constructed using the Topopredict II (35) and HMMTOP (36) programs. The three-dimensional diagram showing the recently reported structure of Ec-NhaA (22) in relation to the functionally important residues of Vc-NhaD was prepared using VMD (44).

Immunodetection of Vc-NhaD in Membranes—Polyclonal anti-NhaD antibodies were produced by Genemed Synthesis, Inc. against the following peptide from a putative IX-X loop of Vc-NhaD: ^{316}AKNDEAALKRIGSVVPFDVFRSISHAC^{342} (with C-terminal cysteine added for coupling). The antibodies were further affinity-purified on the column containing the above peptide coupled to SulfoLink coupling gel (Pierce). The procedure recommended by the manufacturer was followed with a minor modification; the antibodies were eluted in 0.5-ml fractions into Eppendorf tubes containing 50 μl of glycerol and 50 μl of 1 M Tris-HCl, pH 7.5, to prevent antibody precipitation.

To deplete proteins loosely bound to the membranes, aliquots of membrane vesicles containing 100 μg of total membrane protein were carbonate-extracted by the incubation on ice for 15 min in 200 μl of 0.1 M sodium carbonate. The samples were then pelleted by ultracentrifugation at 100,000 rpm in TLA100.3 Beckman rotor for 30 min. The membrane pellets were re-suspended in 200 μl of a standard SDS-PAGE loading buffer each and incubated at 42 °C for 30 min with shaking. For electrophoresis, 20 μl of sample was loaded per lane. Proteins were resolved in 12% polyacrylamide gel and transferred onto a polyvinylidene difluoride Western blotting membrane (Roche Applied Science). The membranes were blocked at room temperature with 10% skim milk powder dissolved in PBS with 1% Tween 20 (Sigma) (PBST) for 30 min. Then the membrane was incubated with the affinity-purified anti-NhaD antibodies at a dilution of 1:3000 in 2% skim milk powder dissolved in PBST. The blot was rinsed 5 times for 5 min each with PBST and incubated for 30 min with goat anti-rabbit IgG horseradish peroxidase conjugate (Bio-Rad) at a dilution of 1:3000 in 2% skim milk powder dissolved in PBST. The blot was rinsed 5 times for 5 min each with PBST. Immunoreactive proteins were visualized using the Amersham enhanced chemiluminescence kit as recommended by the manufacturer. A Fluoro Chem™ 8900 was used to detect the resulting signal.

RESULTS

Strategy of Mutagenesis—Fig. 1*A* illustrates the strategy adopted for choosing the target amino acids for mutagenesis. It shows partial alignments of representative NhaD-like proteins from different organisms. Sequences presented in Fig. 1*A* may be divided into three subgroups, with proteins within subgroups sharing higher degrees of identity/similarity. The largest one includes NhaD-like proteins from bacteria that are free-living or have a free-living stage in their life cycle (Subgroup 1, *last seven rows* in Fig. 1*A*). Chlamydial proteins (from obligate intracellular parasites, *rows three and four* in Fig. 1) comprise the second subgroup (Subgroup 2). The third subgroup includes NhaD from nitrogen-fixing symbiont *Bradyrhizobium japonicum* and higher plant *Arabidopsis thaliana*.

Thirteen polar/charged residues are conserved in all aligned sequences (*highlighted* and marked by *asterisks* in Fig. 1). In Vc-NhaD these residues are Ser-150, Asp-154, Asn-155, Thr-157, Asn-189, Asp-199, Thr-201, Thr-202, Ser-389, Asp-393, Asn-394, Ser-425, and Ser-431. From this list we had previously mutagenized Asp-393 (30) in a study that also included Glu-100, Glu-342, Asp-344, and Thr-345, which are conserved in antiporters belonging to Subgroup 1 as well as

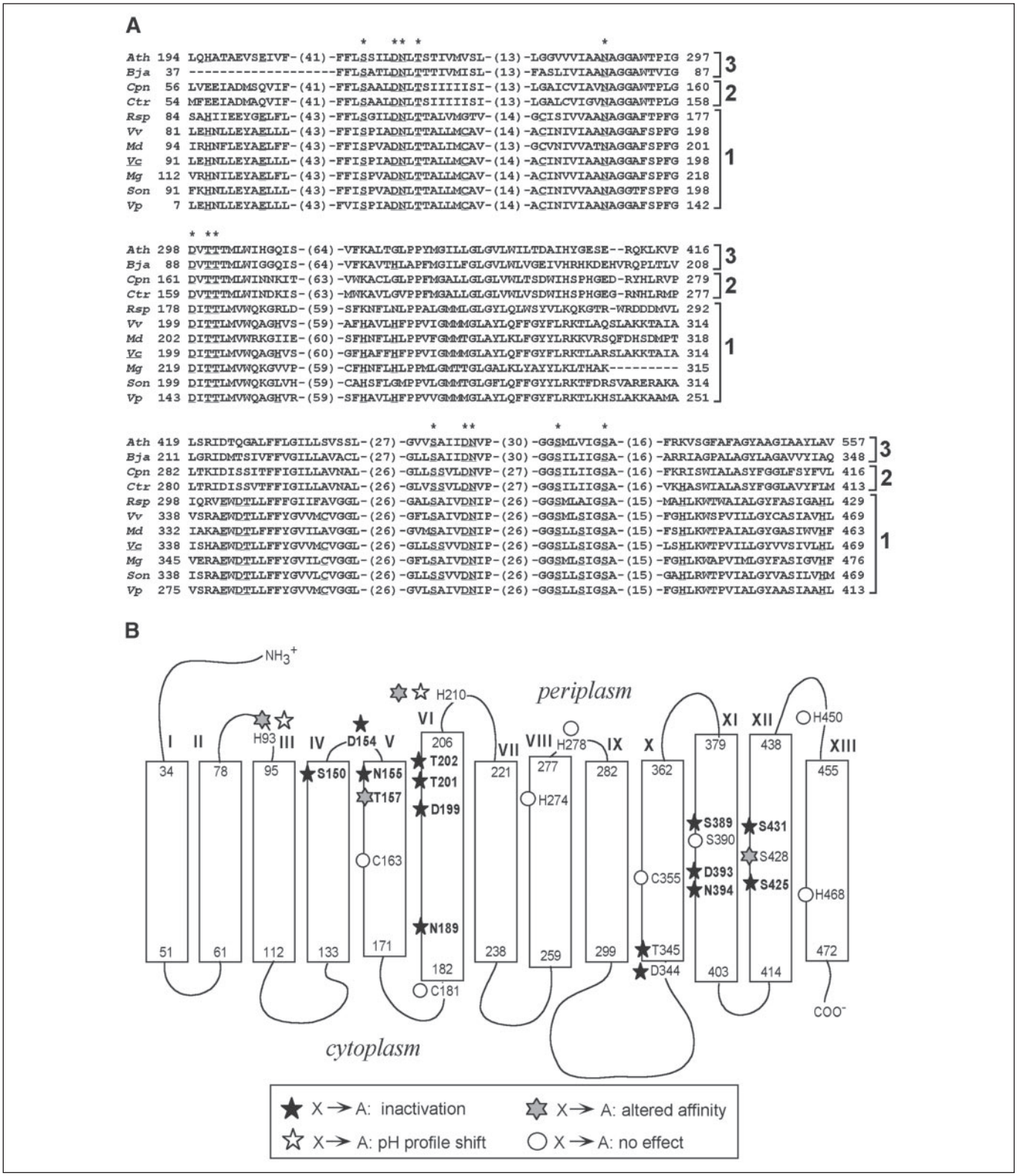

FIGURE 1. ***In silico* analysis of Vc-NhaD.** *A*, partial alignments of representative NhaD proteins. Amino acid sequence of the protein from *A. thaliana* (*Ath*, accession number AAG51773) was used as a query for BLAST. The sequences used were found in *Microbulbifer degradans* (*Md*, ZP_00064921), *Rhodobacter sphaeroides* (*Rsp*, ZP_00007535), *Shewanella oneidensis* (*Son*, AAN54009), *V. cholerae* (*Vc*, AAF96911), *V. parahemeolyticus* (*Vp*, BAC61394), *Vibrio vulnificus* (*Vv*, AAO08110), *Magnetococcus* sp. (*Mg*, ZP_00288831), *Chlamyidophila pneumoniae* (*Cpn*, BAA99222), *Chlamydia trachomatis* (*Ctr*, AAC68454), and *B. japonicum* (*Bja*, NP_770379). Conserved residues targeted for mutagenesis in Vc-NhaD are *underlined*; the *asterisks* (*) indicates polar residues conserved in all aligned sequences. Numbers *1*, *2*, and *3* on the *right side* indicate 3 subgroups of proteins sharing a high degree of identity/similarity (see the text for further details). *B*, distribution of probed residues in the putative transmembrane segments of Vc-NhaD molecule. Conserved residues were generally mutated into alanines, excluding Asp-154 and Asn-394, which were mutated into glycines. Cys-163, Cys-181, and Cys-355 were substituted by serine residues. Strongly conserved residues (that is, conserved in all sequences aligned in Fig. 1) are given in *boldface*. Shown also are functionally important residues Asp-344, Thr-345, and Asp-393 characterized previously (28).

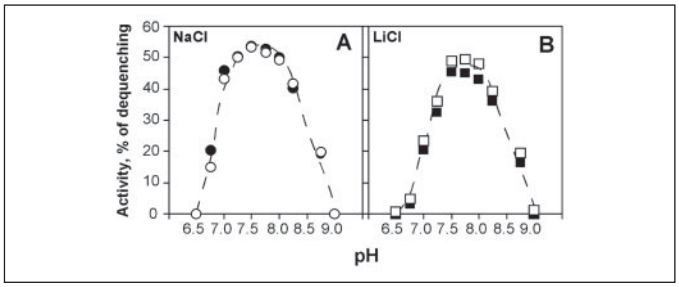

FIGURE 2. **Cys-less variant of Vc-NhaD retains the activity and pH profile of the wild type antiporter.** Sub-bacterial vesicles from EP432 cells expressing either non-mutated Vc-NhaD (*open symbols*) or its Cys-less variant (*closed symbols*) were isolated as described under "Experimental Procedures" and assayed at different pH with 10 mM NaCl (*circles*) or 10 mM LiCl (*squares*). Experiments were repeated at least three times, and results were nearly identical.

the weakly conserved Glu-251. The remaining residues were investigated in this study. Routinely, a target residue was changed into Ala, except Asp-154 and Asn-394, which were changed into Gly. Because our aim was to eliminate charged side chains in chosen positions, either substitution seemed appropriate. Choice of Gly in two mentioned cases just simplified the screening of mutant clones by restriction analysis.

In addition to the fully conserved residues, six His residues, His-93, His-210, His-274, His-278, His-450, and His-468, are conserved at least partially in proteins belonging to Subgroup 1 (Fig. 1*A*). They could have a role in determining the pH response of the antiporter because of their physiologically relevant pK_a. Indeed, mutation of conserved His-225 in Ec-NhaA alters the pH response of the antiporter (15–16). Finally, Vc-NhaD has only three Cys residues, Cys-163, Cys-181, and Cys-355, which are all conserved in Subgroup 1 (Fig. 1*A*). Because the Cys-less variant of Ec-NhaA is nearly as active as wild type protein (17, 21), the Cys residues of Vc-NhaD were also targeted for analysis.

Cys-less Variant of Vc-NhaD Retains Normal Activity—After insertion of the C163S, C181S, and C355S mutations into *nhaD* gene, the mutated gene on the plasmid pTM was introduced into the Na^+/H^+ antiport-deficient EP432 cells of *E. coli*. The EP432/pTM transformants were able to grow in LBK medium supplemented with 100 mM LiCl, which kills untransformed EP432 (data not shown), indicating that the Cys-less Vc-NhaD complemented the EP432 phenotype. Further examination of activity of the Cys-less Vc-NhaD in inside-out membrane vesicles derived from EP432/pTM showed that it is nearly identical to that of the wild type protein with both Na^+ and Li^+ (Fig. 2). Thus, as in the case of phylogenetically distant Ec-NhaA (17, 21), all cysteines in Vc-NhaD can be replaced without loss of function.

Mutagenesis of Conserved His Residues—Fig. 3 summarizes the results of substituting the conserved His residues in Vc-NhaD with Ala. In inside-out sub-bacterial vesicles, H274A, H278A, H450A, and H468A did not change the $Na^+(Li^+)/H^+$ antiport activity significantly, but H93A and H210A variants displayed an acidic shift of the pH profile of the antiport for both alkali cations (Fig. 3). The shift was more pronounced in the H93A variant, which also responded differently to Na^+ and Li^+ ions, showing higher activity with Li^+ (Fig. 3). To further assess the affinity of H93A and H210A variants to alkali cations, the concentrations of Na^+ and Li^+ required for half-maximal response (apparent K_m values) at pH 7.75 were determined in sub-bacterial vesicles (TABLE ONE). Despite the fact that apparent K_m is only indirectly related to the actual K_m of the antiporter, this readily measurable parameter is commonly used to characterize antiporter affinity to substrate ions (for example, see Ref. 14). Here again the apparent K_m of H93A for Na^+ was ~7-fold higher than in the wild type, whereas its apparent K_m for Li^+ was unaffected (TABLE ONE). By contrast, there was only a slight increase in the apparent K_m of H210A for Li^+ (TABLE ONE).

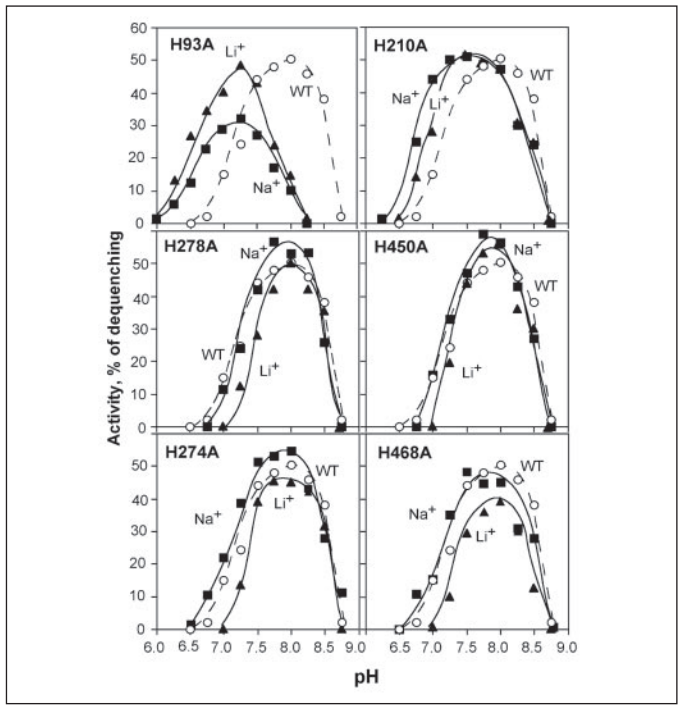

FIGURE 3. **Effect of His → Ala substitutions on the pH profile of activity of Vc-NhaD.** Experimental conditions are as in Fig. 2. Activity of the wild type (*WT*) Vc-NhaD with 10 mM NaCl is shown for the reference (*empty circles*). All measurements were repeated at least three times, and results were essentially the same.

TABLE ONE

Affinity of different Vc-NhaD variants to alkali cations

Mutation	Apparent K_m (pH 7.75)	
	Na^+	Li^+
	mM	
Wild type	1.1	2.1
S390A	1.1	2.1
T157A	9.5	39.8
S428A	5.5	17.9
H93A	7.1	1.9
H210A	1.3	4.3

Conserved Polar Residues Associated with Putative Transmembrane Segments IV, V, and VI Are Functionally Important—Computer modeling of the Vc-NhaD membrane topology suggests that the highly conserved residues Ser-150, Asp-154, Asn-155, Thr-157, Asp-199, Thr-201, and Thr-202 may form a compact "constellation" on the periplasmic side of the protein (see Fig. 1*B*). Variants S150A, D154G, N155A, D199A, T201A, T202A, and N189A failed to complement the Li^+-sensitive growth phenotype in EP432 (TABLE TWO), and analysis of activity in sub-bacterial vesicles confirmed that they were unable to mediate the Na^+- and Li^+-dependent H^+ transport at pH 6.5–8.75 (Fig. 4 and data not shown). Immunodetection confirmed that this was not due to the impaired expression and/or targeting of mutant variants (Fig. 5). EP432 cells expressing the T157A variant showed slower growth in the presence of 100 mM LiCl (TABLE TWO). The T157A variant also exhibited lower activity in vesicle assays (Fig. 4, *A–B*) and a decreased affinity for alkali cations (TABLE ONE). Furthermore, the comparison of apparent K_m values revealed a difference in responses of the mutated antiporter to alkali cations with Na^+ becoming the preferred substrate (TABLE ONE).

TABLE TWO

Growth of EP432 cells expressing different Vc-NhaD variants in the LBK medium supplemented with 100 mM LiCl at 37 °C

Variant expressed	Doubling time
	min
None ("empty" vector)	>300
Wild type	38
S390A	37
T157A	79
S428A	60
S150A, D154G, N155A, N189A, D199A, T201A, T202A, S389A, N394G, S428A, S431A	>300

Analysis of Conserved Polar Residues in Putative TMS XI and XII—Previously we found that Asp-393 in TMS XI as well as Asp-344 and Thr-345 at the cytoplasmic end of TMS X are functionally important (30). Another four nearby polar/charged residues are conserved in NhaD antiporters (Fig. 1*A*), including Ser-389 and Asn-394 in TMS XI as well as Ser-425 and Ser-431 in TMS XII. In addition, Ser-428 is conserved in proteins belonging to Subgroup 1, whereas Ser-390 is replaced by alanine in many cases (Fig. 1*A*). These residues were mutagenized to alanine (except Asn-394, which was replaced by glycine), and the antiport activities were assayed in sub-bacterial vesicles of transformed EP432 (Fig. 4). The activity of the S390A variant was unaffected compared with native protein (Fig. 4, *E–F*), but mutation of conserved Ser-389, Asn-394, Ser-431, and Ser-425 prevented $Na^+(Li^+)$-dependent H^+ transfer in vesicles completely (Fig. 4 and data not shown). The S428A and T157A variants displayed similar slow growth of EP432 transformants in LiCl-containing medium (TABLE TWO), lowered activity in vesicles (Fig. 4, *C–D*), and different response to Na^+ and Li^+. K_m of S428A for Na^+ was 5.5 times higher than that of the wild type antiporter, whereas its K_m for Li^+ was almost 9-fold elevated (TABLE ONE).

Expression/Targeting of Vc-NhaD Variants—Because a number of Vc-NhaD variants were unable to complement the EP432 phenotype and catalyze $Na^+(Li^+)$-dependent H^+ transfer in sub-bacterial vesicles, levels of their expression in the EP432 membranes were examined by Western blotting. It confirmed that the mutations generally did not interfere with either the expression or targeting to the membrane (Fig. 5). Expression levels of all inactive variants in EP432 except S431A were comparable with that of the wild type protein, and even for S431A the slightly reduced levels cannot account for the complete absence of activity.

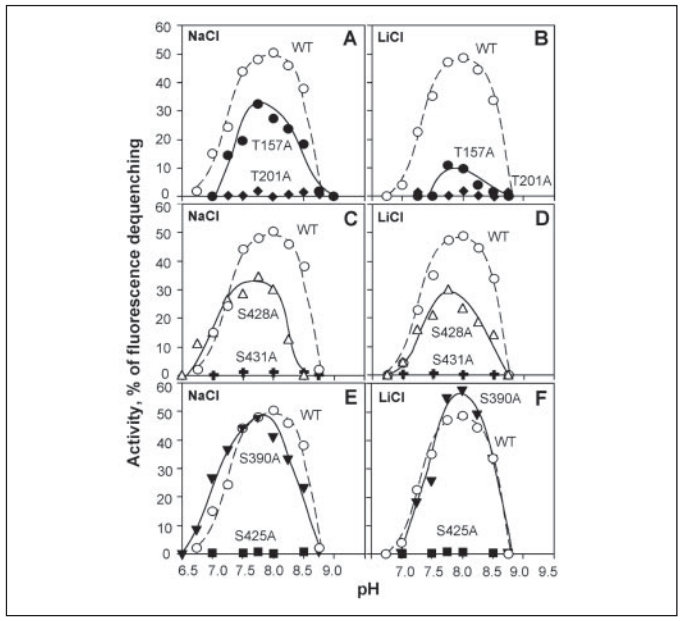

FIGURE 4. **The pH profiles of different variants of Vc-NhaD determined in everted sub-bacterial vesicles of EP432 expressing the corresponding variant.** Experimental conditions are as in Fig. 2. T201A, S431A, and S425A exemplify mutations such as S150A, D154G, N155A, T202A, D199A, S389A, and N394G that resulted in a complete arrest of the Na^+-dependent H^+ transfer in vesicles over the pH range 6.6–9.0. All experiments were repeated at least three times, and results were nearly identical. *WT*, wild type.

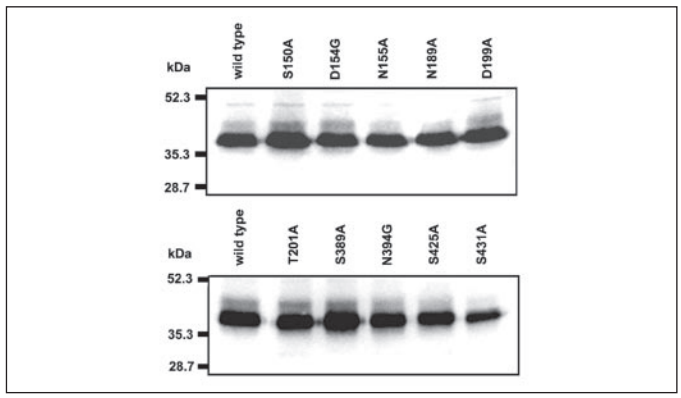

FIGURE 5. **Immunodetection of different variants of Vc-NhaD in the membranes of EP432.** Neither mutation prevented the expression and targeting of the antiporter. The level of the expression of T202A variant was very similar to that of T201A (not shown). Western blot analysis with affinity purified polyclonal anti-Vc-NhaD antibodies was performed as described under "Experimental Procedures."

DISCUSSION

The present study is the first to provide an extensive molecular analysis of a Na^+/H^+ antiporter of the NhaD type. General methodology of the analysis of mutant variants of Na^+/H^+ antiporters has been developed over the past decade, primarily in works by Padan and co-workers (see, for example, Refs. 20 and 37). This methodology allows the differentiation among residues that regulate the pH response of an antiporter and those involved in the translocation of cations. The former residues are expected to (i) have a p*K* in the physiological pH range, (ii) change the pH profile of antiport when mutated without an effect on the K_m of antiport, and (iii) maintain the altered pH profile of a mutant variant assayed at saturating concentrations of substrate alkali cations. In terms of function, such residues could form an allosteric "built-in pH sensor" (20, 37) or belong to the intramolecular H^+ translocation pathway. The latter residues should (i) be associated with transmembrane segments, (ii) be able to interact with translocated cations, and (iii) affect the K_m of antiport when mutated without affecting the wild type pH profile, at least at saturating concentrations of alkali cations. Obviously, such residues could affect ion translocation either directly (*i.e.* by providing ligands for the coordination of transported cations) or indirectly (being important for the overall protein structure or conformational changes associated with ion translocation without direct interaction with substrate cations). Finally, some residues might be involved in both the pH response and ion translocation, for example if protons and alkali cations share at least some segments of the same translocation pathway.

Applying the above criteria to the functionally important residues identified in Vc-NhaD, one can classify Ser-150, Asp-154, Asn-155, Asn-189, Asp-199, Thr-201, Thr-202, Asp-344, Thr-345, Ser-389, Asp-393, Asn-394, Ser-425, and Ser-431 as ones involved either directly or indirectly in ion translocation. All these residues are either polar or charged and, thus, can coordinate or repel cations. They are located within hydrophobic segments of Vc-NhaD or at the membrane-water interface. Mutation of any of them arrests the overall reaction of cation-

proton antiport over a pH range from 6.0 to 9.0. This is not due to the interference of mutations with expression/targeting (Fig. 5). Although a somewhat lowered level of variant S431A in the membranes was detected (Fig. 5), it far exceeded the expression of Vc-NhaD from its chromosomal gene in *V. cholerae*.[4] A very low abundance is one of characteristic features of bacterial Na^+/H^+ antiporters. For example, Ec-NhaA, the major antiporter of *E. coli*, remains immunochemically undetectable in the membrane unless it is overexpressed in *trans* (45). Therefore, it seems highly unlikely that impaired expression or targeting is the reason for the lack of activity of S431A. Furthermore, it definitely cannot account for the difference in responses of T157A and S428A to Na^+ and Li^+ (Fig. 4). Most likely, it is the altered affinity of these variants to alkali cations that causes their lowered activity (TABLE ONE). It is significant that these residues are all evolutionarily conserved (Fig. 1*A*), whereas Ser-390 is replaced by alanine in a number of NhaD proteins (Fig. 1*A*). Not surprisingly, Ser-390 is not essential for the activity of Vc-NhaD. Its substitution by alanine does not affect either the pH profile of activity (Fig. 4, *E–F*) or apparent K_m for alkali cations (TABLE ONE).

Charged/polar residues associated with TMSs have been implicated in the ion translocation mediated by a variety of Na^+-dependent transporters. The Na^+-binding sites of the Na^+ motive ATPases from *Propionigenium modestum* and *Acetobacterium woodii* are thought to be formed by closely positioned conserved Asp, Thr, and Asn residues (38–39). Hydroxyl groups provided by Ser and Thr residues are critical for activity of such diverse Na^+-motive proteins as the proline transporter in *E. coli* (40), the Na^+-dependent oxaloacetate decarboxylase (41), the Na^+/iodide symporter (42), and the glutamate transporter GLT-1 (43). Most importantly, recent analysis of the structure of Ec-NhaA clearly shows that Asp-163, Asp-164, and Thr-132 are parts of the catalytic site in this bacterial Na^+/H^+ antiporter (22). Two residues definitely involved in the alkali cation binding and/or translocation, Thr-157 and Ser-428, are located in the TMSs V and XII, respectively (Fig. 1*B*), and variants of both show markedly lower affinity to Li^+ compared with Na^+ (Fig. 4 and TABLE ONE), supporting the idea of Li^+ having more stringent structural requirements for binding to the antiporter.

Functionally important amino acids identified in Vc-NhaD form three major clusters (Fig. 1*B*). Cluster 1 includes Ser-150, Asp-154, Asn-155, Thr-157, Asp-199, Thr-201, and Thr-202 in neighboring TMS IV, V, and VI. Cluster 2, presumably located at the opposite side of the transmembrane segments, includes Asp-344 and Thr-345 in TMS X (30). Finally, Cluster 3, located in the middle of TMSs XI-XII, includes Ser-389, Asp-393, Asn-394, S425, Ser-428, and Ser-431. This distribution presents distinct parallels to the recently reported structure of Ec-NhaA resolved at 3.45 Å (22), which provides important insights into function of bacterial Na^+/H^+ antiporters. In particular, a negatively charged funnel with Glu-78, Glu-82, Glu-252, and Asp-11 at its entrance leads from the cytoplasm to a putative catalytic site in the middle of the membrane containing the charged/polar residues Asp-163, Asp-164, Thr-132, and Asp-133. On the opposite side of the protein, a shallow, negatively charged funnel with Asp-65 at its tip connects the periplasm to the central cation-binding site (22). The arrangement allows for the access of substrate ions through the funnels to the catalytic site, which could operate in the alternating-access mode (22). It is tempting to speculate that phylogenetically unrelated Vc-NhaD shares these structural elements. Cluster 1 in TMSs IV-VI together with His-93 and His-210 may represent an analog of the shallow negatively charged funnel on the periplasmic side of Ec-NhaA, attracting cations toward the putative catalytic site in the middle of the protein made up of Cluster 2 in TMSs XI and XII. Of note, five or six oxygen ligands are required to coordinate an alkali cation (46–47) and residues of Cluster 2, Ser-389, Asp-393, S425, Ser-428, and Ser-431 will suffice in this respect. Finally, the pair of Asp-344 and Thr-345 on TMS X and Asn-189 of TMS VI may be part of the funnel that facilitates the ion access from the cytoplasmic side. Thus, despite their distant phylogenetic relationships, different groups of bacterial Na^+/H^+ antiporters may share common structural features and catalytic mode. Possible similarities between Ec-NhaA and Vc-NhaD outlined above are summarized in Fig. 6. It should be stressed here though that a crystal structure of Vc-NhaD is required to determine the location of each residue.

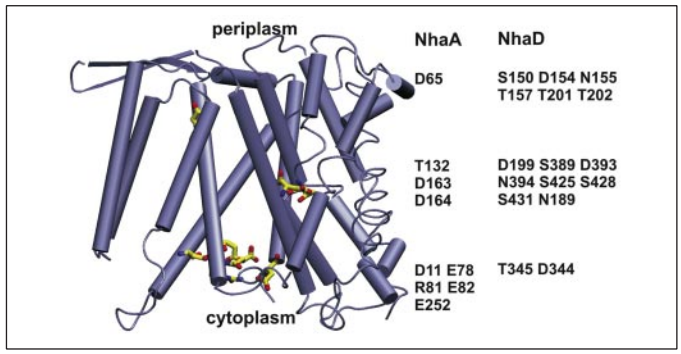

FIGURE 6. **Possible analogies between functionally important residues in Ec-NhaA and Vc-NhaD.** The structure of Ec-NhaA is shown on the *left* along with a listing of conserved residues known to have a role in antiport. A listing of residues from Vc-NhaD in equivalent positions is included on the *right*. In both cases a group of negatively charged/polar residues in the middle of the structure might form the putative cation-binding site with two other groups at opposite sides facilitating the access of ions to this active site.

Of all conserved residues examined, only His-93 and His-210 contribute to the pH response of Vc-NhaD (Fig. 3). Interestingly, these histidines are located in short periplasmic loops flanking Cluster 1 of functionally important residues in TMS IV-VI (Fig. 1*B*). The acidic shift of the pH profile of activity in these variants can be explained by the protonatable side chains of these residues being involved in initial H^+ binding, such that their elimination results in a higher concentration of protons required for maximal activity. On the other hand, the effect of H210A and H93A mutation on the apparent K_m for alkali cations suggests that these residues also contribute to the coordination of Na^+ (in the case of His-93) or Li^+ (His-210) instead of H^+ at some stage of the catalytic cycle. The effects of mutations in His-93, His-210, and in residues of cluster 1 are in accord with the concept that periplasmic parts of TMSs IV-VI together with flanking loops form a funnel with low selectivity that channels substrate cations toward the putative catalytic site associated with TMSs XI-XII.

The distribution of functionally important residues in the Vc-NhaD molecule suggests that two groups of transmembrane segments, TMSs IV-VI and TMSs X-XII, may be located close to one another. Because the Cys-less variant of Vc-NhaD is fully active (Fig. 2), the helical packing of Vc-NhaD as well as the precise membrane topology of the antiporter may be probed by Cys-scanning mutagenesis. In particular, introducing pairs of Cys residues at appropriate locations and applying different cross-linking reagents, one may estimate the distances between TMSs of interest. This work is currently under way.

Acknowledgment—Many thanks are due to Dr. T. A. Krulwich for critical reading of the manuscript and valuable suggestions.

[4] J. Dzioba, unpublished observation.

REFERENCES

1. Busch W., and Saier, M. H., Jr. (2002) *Crit. Rev. Biochem. Mol. Biol.* **37,** 287–337
2. Padan, E., and Schuldiner, S. (1992) in *Alkali Cation Transport Systems in Procaryotes* (Bakker, E., ed) pp. 3–24, CRC Press, Inc., Boca Raton, FL
3. Padan, E., and Schuldiner, S. (1994) *Biochim. Biophys. Acta* **1185,** 129–151
4. Padan, E., Venturi, M., Gerchman, Y., and Dover, N. (2001) *Biochim. Biophys. Acta* **1505,** 144–157
5. Goldberg, B. G., Arbel, T., Chen, J., Karpel, R., Mackie, G. A., Schuldiner, S., and Padan, E. (1987) *Proc. Natl. Acad. Sci. U. S. A.* **84,** 2615–2619
6. Pinner, E., Padan, E., and Schuldiner, S. (1992) *J. Biol. Chem.* **267,** 11064–11068
7. Padan, E., Maisler, N., Taglicht, D., Karpel, R., and Schuldiner, S. (1989) *J. Biol. Chem.* **264,** 20297–20302
8. Pinner, E., Kotler, Y., Padan, E., and Schuldiner, S. (1993) *J. Biol. Chem.* **268,** 1729–1734
9. Taglicht, D., Padan, E., and Schuldiner, S. (1991) *J. Biol. Chem.* **266,** 11289–11294
10. Pinner, E., Padan, E., and Schuldiner, S. (1994) *J. Biol. Chem.* **269,** 26274–26279
11. Taglicht, D., Padan, E., and Schuldiner, S. (1993) *J. Biol. Chem.* **268,** 5382–5387
12. Dibrov, P., and Taglicht, D. (1993) *FEBS Lett.* **336,** 525–529
13. Dibrov, P. (1993) *FEBS Lett.* **336,** 530–534
14. Gerchman, Y., Rimon, A., Venturi, M., and Padan, E. (2001) *Biochemistry* **40,** 3403–3412
15. Gerchman, Y., Olami, Y., Rimon, A., Taglicht, D., Schuldiner, S., and Padan, E. (1993) *Proc. Natl. Acad. Sci. U. S. A.* **90,** 1212–1216
16. Rimon, A., Gerchman, Y., Olami, Y., Schuldiner, S., and Padan, E. (1995) *J. Biol. Chem.* **270,** 26813–26817
17. Olami, Y., Rimon, A., Gerchman, Y., Rothman, A., and Padan, E. (1997) *J. Biol. Chem.* **272,** 1761–1768
18. Inoue, H., Noumi, T., Tsuchiya, T., and Kanazawa, H. (1995) *FEBS Lett.* **363,** 264–268
19. Noumi, T., Inoue, H., Sakurai, T., Tsuchiya, T., and Kanazawa, H. (1997) *J. Biochem.* **121,** 661–670
20. Galili, L., Rothman, A., Kozachkov, L., Rimon, A., and Padan, E. (2002) *Biochemistry* **41,** 609–617
21. Rimon, A., Tzubery, T., Galili, L., and Padan, E. (2002) *Biochemistry* **41,** 14897–14905
22. Hunte, C., Screpanti, E., Venturi, M., Rimon, A., Padan, E., and Michel, H. (2005) *Nature* **435,** 1197–1202
23. Tzuberi, T., Rimon, A., and Padan, E. (2004) *J. Biol. Chem.* **279,** 3265–3272
24. Heidelberg, J. F., *et al.* (2000) *Nature* **406,** 477–483
25. Krulwich, T. A., Jin, J., Guffanti, A. A., and Bechhofer, D. H. (2001) *J. Mol. Microbiol. Biotechnol.* **3,** 237–246
26. Pragai, Z., Eschevins, C., Bron, S., and Harwood, C. R. (2001) *J. Bacteriol.* **183,** 2505–2515
27. Kosono, S., Ohashi, Y., Kawamura, F., Kitada, M., and Kudo, T. (2000) *J. Bacteriol.* **182,** 898–904
28. Southworth, T. W., Guffanti, A. A., Moir, A., and Krulwich, T. A. (2001) *J. Bacteriol.* **183,** 5896–5903
29. Dzioba, J., Ostroumov, E., Winogrodzki, A., and Dibrov, P. (2001) *Mol. Cell. Biochem.* **229,** 119–124
30. Ostroumov, E., Dzioba, J., Loewen, P. C., and Dibrov, P. (2002) *Biochim. Biophys. Acta* **1564,** 99–106
31. Nozaki, K., Kuroda, T., Mizushima, T., and Tsuchiya, T. (1998) *Biochim. Biophys. Acta* **1369,** 213–220
32. Häse, C., Fedorova, N., Galperin, M. Y., and Dibrov, P. (2001) *Microbiol. Mol. Biol. Rev.* **65,** 353–370
33. Dibrov, P., Dibrov, E., Pierce, G. N., and Galperin, M. Y. (2004) *J. Mol. Microbiol. Biotechnol.* **8,** 1–6
34. Altschul, S., Madden, T., Schaffer, A., Zhang, J., Zheng, Z., Miller, W., and Lipman, D. (1997) *Nucleic Acids Res.* **25,** 3389–3402
35. Claros, M., and von Heijne, G. (1994) *Comput. Appl. Biosci.* **10,** 685–686
36. Tusnády, G. E., and Simon, I. (1998) *J. Mol. Biol.* **283,** 489–506
37. Padan, E., Tzubery, T., Herz, K., Kozachkov, L., Rimon, A., and Galili, L. (2004) *Biochim. Biophys. Acta* **1658,** 2–13
38. Kaim, G., Wehrle, F., Gerike, U., and Dimroth, P. (1997) *Biochemistry* **36,** 9185–9194
39. Rahlfs, S. M. V. (1997) *FEBS Lett.* **404,** 269–271
40. Quick, M., Tebbe, S., and Jung, H. (1996) *Eur. J. Biochem.* **239,** 732–736
41. Jockel, P., Schmid, M., Steuber, J., and Dimroth, P. (2000) *Biochemistry* **39,** 2307–2315
42. De La Vieja, A., Dohan, O., Levy, O., and Carrasco, N. (2000) *Physiol. Rev.* **80,** 1083–1105
43. Zhang, Y., and Kanner, B. I. (1999) *Proc. Natl. Acad. Sci. U. S. A.* **96,** 1710–1715
44. Humphrey, W., Dalke, A., and Schulten, K. (1996) *J. Mol. Graph.* **14,** 33–38
45. Rimon A., Gerchman Y., Kariv Z., and Padan, E. (1998) *J. Biol. Chem.* **273,** 26470–26476
46. Glusker, G. P. (1991) *Adv. Protein Chem.* **42,** 1–76
47. Harding, M. M. (2004) *Acta Crystallogr. D Biol. Crystallogr.* **60,** 849–859